MICROSTRUCTURE AND MECHANICAL PROPERTIES OF A SINTERED DUAL PHASE STEEL OBTAINED FROM A MIXTURE OF 316L AND 434L STAINLESS STEEL POWDERS

T. Marcu, M. Pellizzari, J. Kazior, T. Pieczonka, S. Gialanella, A. Molinari

Abstract

The microstructural evolution caused by solubilization heat treatments of a dual phase sintered stainless steel was investigated and correlated to tensile and impact properties. Mechanical properties depend on the martensite content, which in turn depends on the treatment temperature. In particular, it has been observed that an increase in the treatment temperature reduces martensite content. The material solubilized at 1100°C resulted to be the one with better mechanical properties, as the best combination of strength, ductility and impact properties was attained.

Keywords: stainless steel powders, microstructure, mechanical properties, impact test

INTRODUCTION

In order to produce a duplex stainless steel using commercial powders, mixtures of austenitic and ferritic powders, with different ferrite/austenite ratio were compacted and sintered [1, 2]. Due to the non-equilibrium condition of the mixtures, sintering is accompanied by microstructural changes that modify the phase composition of the material. Nickel diffusion from austenite to ferrite causes the destabilization of austenite, which transforms on cooling from the sintering temperature into a novel phase that will be referred to as the "new constituent". Therefore, the austenite content of the sintered products is lower than in the starting mixtures. An additional effect is the enhanced densification, if compared to that displayed by the two powders processed under the same conditions [3].

Corrosion resistance of these materials is comparable to that of the two monophase steels and is very much affected by the open porosity [2]. In this respect, the enhancement of densification has a positive effect on corrosion resistance.

Mechanical properties depend on the microstructure, which in turn depends on the composition of the starting mixture. The new constituent is harder than ferrite and austenite and has a very fine microstructure. It increases strength and reduces ductility of the sintered materials. In particular, the alloy containing 75 % of ferritic powder in the starting mixture reaches UTS over 500 MPa, $\sigma_{y0.2}$ of about 400 MPa with elongation at failure of about 1 %, at 6.8 g/cm^3 density. In this case, the sintered alloy comprises 70 % ferrite and 30 % of the new constituent.

The properties displayed by these alloys are potentially interesting for those applications where corrosion resistance of an austenitic stainless steel would be required in combination with a high tensile strength.

Teodora Marcu., Massimo Pellizzari, Sefano Gialanella, Alberto Molinari, University of Trento, Trento, Italy
Jan Kazior, Cracow Technical University, Cracow, Poland
Tedeusz Pieczonka, Academy of Mining and Metallurgy, Cracow, Poland

High strength duplex stainless steels are usually produced by ingot metallurgy. For instance Miyakusu et al. [4] have tried to apply intercritical annealing to ferritic stainless steel, and developed 17 % Cr - 1.5 % Ni ferrite-martensite dual-phase stainless steel sheets, having good formability as well as high strength. In this process, the hot-rolled and annealed sheets were subsequently cold-rolled and then annealed in the single phase ferritic region. These sheets, which consisted of ferrite single phase, were air-cooled and finally annealed in the ferrite austenite two-phase region, followed by air-cooling. During air cooling, austenite transforms into martensite. By this treatment, a fine duplex structure consisting of ferrite and martensite, is obtained, which exhibits an excellent strength-elongation balance as compared to conventionally tempered cold-rolled sheets of ferritic stainless steel [5].

Another transformation observed in the investigated materials is the precipitation of sigma phase, occurring on cooling from the sintering temperature. It is well known that sigma phase reduces corrosion resistance and causes brittleness. Any attempt to eliminate sigma phase by fast cooling from the sintering temperature failed, and therefore a solubilization treatment is needed. Material has to be heated up to a temperature in the range 1000-1200°C, held at that temperature to completely dissolve sigma phase and quenched into water to avoid any further re-precipitation.

In view of the promising overall properties of the 75 % ferritic material, the research was continued to investigate the effect of heat treatments on the alloy microstructure. Solubilization treatments were carried out at different temperatures. The microstructural changes brought about by heat treatments were investigated by different microscopy techniques. The new constituent, coming from austenite destabilization, was analysed. Tensile and impact properties were determined, as well.

EXPERIMENTAL PROCEDURE

The starting raw material consists of a 25 %/75 % mixture, codenamed "75F", of water atomised 316L and 434L stainless steel powders, whose chemical compositions are given in Table 1.

Tab.1. Chemical compositions of the base powder (% wt.).

Powder	Cr	Ni	Mo	Mn	Si	C	Fe
AISI 316L	16.3	12.75	2.28	0.17	0.87	0.019	Bal.
AISI 434L	16.57	-	1.03	0.18	0.70	0.016	Bal.

Green compacts, pressed at 600 MPa in a uniaxial press, were sintered at 1240°C for 1 hour in H_2 atmosphere and cooled at 80°C/min down to 600°C at 10°C/min.up to 20°C. Both tensile (ISO 2470) and impact Charpy (ISO 5745) specimens were prepared. Density, measured by the water displacement method, was of 6.93 g/cm^3; open porosity was 8 %.

To dissolve sigma phase, solubilization treatments were performed at three different temperatures: 1000°C, 1100°C and 1200°C, for one hour. Each treatment was followed by water quenching. These treatments were carried out in a tubular laboratory furnace, under a protective Ar flow.

Microstructural analyses were carried out by Optical Microscopy (OM) and the Scanning Electron Microscopy (SEM) observations. Beraha I (0.7 g $K_2S_2O_5$, 20 ml HCl, 100 ml water) reagent was used for metallographic etching. The distribution of alloying elements in the different phases was determined by energy dispersive x-ray spectroscopy (EDXS). The percentages, morphology and grain size of different phases were determined

by Image Analysis at the optical microscope, on five representative fields. To individuate the new constituent formed on sintering, transmission electron microscopy (TEM) observations and selected area diffraction (SAD) analyses were carried out. The specimens were thinned to electron transparency with the following procedure: starting from 1 mm thick disks, they were mechanically ground down to 70 microns. For the final thinning a twin jet electropolisher, operated at 15 V and 35 mA, was used with a 90 % ethanol – 10 % perchloric acid etching solution kept at -1°C.

Tensile tests were carried out on an Instron apparatus, with a cross head speed of 1 mm/min. Instrumented impact tests were carried out on a Charpy pendulum, with an available energy of 150 J and an impact speed of 3.9 m/sec.

RESULTS AND DISCUSSION

Microstructure of as-sintered 75F

Figure 1 shows the microstructure of as-sintered material, consisting of ferrite (bright grey phase) and the new constituent (dark grey phase). Quantitative microstructural analysis gives the following constitution: 70 % ferrite, 30 % new constituent.

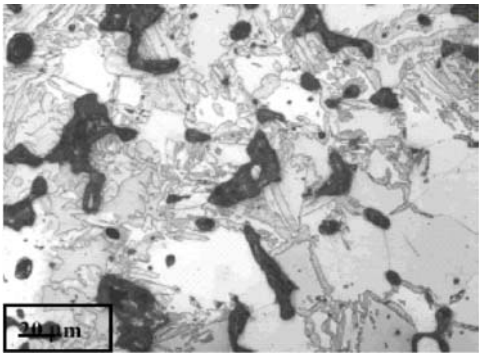

Fig.1. Microstructure of as sintered material.

The new constituent results from the transformation on cooling of interdiffusion zones between austenite and ferrite [1]. During holding at the sintering temperature, Ni diffuses from austenite to ferrite, leading to the formation of regions with intermediate composition between those of ferrite and austenite. On cooling, these regions transform into the new constituent, which contains about 4.5 % Ni, as shown by EDXS analyses [1]

Figure 2 is a TEM bright field image of the specimen. The two grains have a different Ni content: 2 % the bright grain and 4 % the dark grain, as measured by EDXS analyses. On the basis of these analytical data, the two grains are attributed to ferrite (the bright one) and the new constituent (the dark one). Its crystalline lattice is bcc, as shown by SAD (Fig.3), with lattice parameter 0.286 nm. Microhardness is 348 HV0.01 [2]. SEM clearly highlights the lath morphology (Fig.4). The new constituent is a carbon free Fe-Cr-Ni-Mo martensite.

Fig.2. TEM bright field image showing the grain morphology of the two phases present in the material.

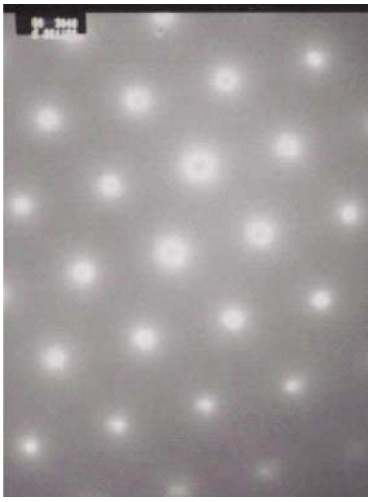

Fig.3. SAD of the region of interest.

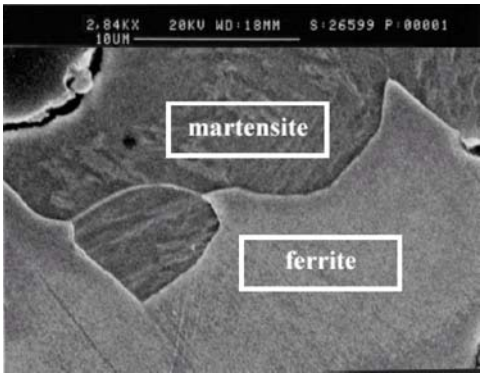

Fig.4. SEM micrograph illustrating the lath morphology of the martensite.

Microstructure of 75F after solubilization at different temperatures

The microstructures of solution treated materials are shown in Figs.5-7. They still consist of ferrite and martensite, present to different extents, according to the treatment temperature.

Sigma phase has been completely eliminated by all heat treatments. In the 1200°C treated material, only a few martensitic areas are visible, dispersed into an equiaxed ferritic matrix. On the other hand, the two other materials show a fine dispersion of the two constituents, very similar to the one obtained by intercritical annealing of dual phase steels [6]. In Table 2 the results of the quantitative microstructural analysis performed by an Image Analyser are listed: ferrite content increases with the treatment temperature, up to 95 % in the 1200°C treated material.

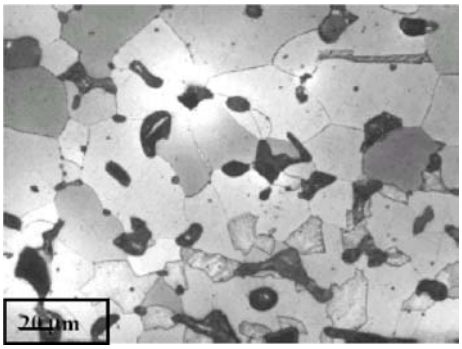

Fig.5. Microstructure of material solubilized at 1200°C.

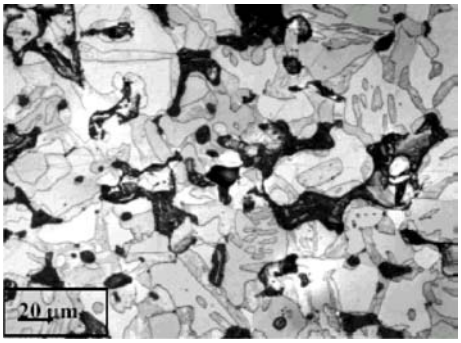

Fig.6 Microstructure of material solubilized at 1100°C.

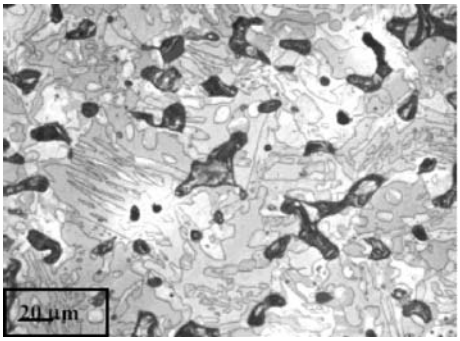

Fig.7. Microstructure of material solubilized at 1000°C.

Tab.2. Phase composition of the studied materials as a function of the treatment temperature.

Tsol. [°C]	% ferrite	% martensite
1200	95	5
1100	70	30
1000	53	47
as sintered	70	30

The microstructure of these materials has been interpreted with the help of the equilibrium phase diagram, calculated by the ThermoCalc program, using the TC-Fe2000 database [7]. The equilibrium diagram was calculated for two different steels, having different molybdenum concentration: 1.03 % (that of the ferritic powder) and 2.28 % (that of the austenitic powder), but the same concentrations of carbon (0.016 %), chromium (16.5 %), silicon (0.76 %, the weighed mean between the concentrations in the ferritic and the austenitic powder) and manganese (0.18 %). Two molybdenum concentrations were adopted, as, according to the EDXS results, no appreciable Mo diffusion occurs during holding at the sintering temperature. Figures 8 and 9 shows the calculated portions of the two diagrams. The evolution of the as-sintered ferrite was followed on the diagram with the lower Mo content (Fig.8), whilst that of the as-sintered martensite was on the other one (Fig.9), since martensite would form on cooling from the destabilized austenitic areas, as previously described.

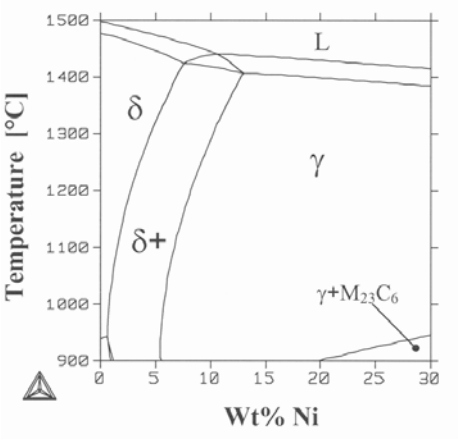

Fig.8. Thermocalc diagram for as sintered ferrite.

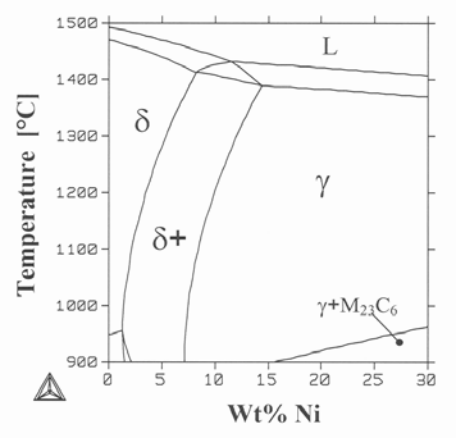

Fig.9. Thermocalc diagram for as sintered martensite.

From the Figures 8-9, the microstructural constituents formed at the three solubilization temperatures by ferrite and martensite were determined and quantified by the lever rule. Results are reported in Table 3.

Tab.3. Phase composition at the treatment temperatures, as determined by ThermoCalc.

Temperature [°C]	As-sintered ferrite (70%)				As-sintered martensite (30%)			
	determined on the diagram		normalized to 70 %		determined on the diagram		normalized to 30 %	
	ferrite [%]	austenite [%]	ferrite [%]	austenite [%]	ferrite [%]	austenite [%]	ferrite [%]	austenite [%]
1000	53.5	46.5	37	33	34.6	65.4	11	19
1100	74	26	52	18	50.2	49.8	15	15
1200	100	0	70	0	78.3	21.7	23	7

In Table 4 the calculated phase percentages of the materials at the three solubilization temperatures are listed. These phase compositions can be compared to the microstructure after each heat treatment. With the assumption that on quenching the amount of ferrite remains unchanged, while austenite transforms into martensite, the agreement between the calculated microstructure and that determined by Image Analysis (Tab.2) is definitely a good one.

Tab.4. Comparison between calculated and real microstructure.

Temperature [°C]	calculated from the equilibrium phase diagram		determined by Image Analysis (Table 2)	
	ferrite [%]	martensite [%]	ferrite [%]	martensite [%]
1000	47	53	53	47
1100	67	33	70	30
1200	93	7	95	5

Mechanical properties

Microhardness and tensile properties (UTS, $\sigma y_{0.2}$, elongation) are listed in Tab.5.

Tab.5. Mechanical properties of as sintered and solubilized materials.

Temperature [°C]	HV0.01	UTS [MPa]	$\sigma_{y\ 0.2}$ [MPa]	A [%]
as sintered	217	516	392	1.1
1000	322	566	479	0.9
1100	284	564	435	1.6
1200	236	488	382	2.2

Apart from the one carried out at 1200°C, all solubilization treatments increase microhardness and tensile strength and decrease elongation and impact energy.

The decrease in strength and the increase in ductility obtained at 1200°C is clearly attributable to the decrease of the martensite content with respect to the as-sintered condition. It is worth saying that the expected improvement in ductility, due to the elimination of sigma phase, is hidden by the microstructural changes.

The microstructure of the material treated at 1200°C makes it more similar to a ferritic rather than a two-phase steel, like the other ones considered in the present investigation.

Table 6 compares the mechanical properties of this material to those of the pure AISI434L steel [2] compacted and sintered under the same conditions. The two-phase material displays a noticeably higher tensile strength, which cannot be simply correlated to a higher density and microhardness, and a lower ductility as compared to pure ferritic steel. The increased strength is due to the enhanced densification and to the reduction of grain size, resulting from heat treatment (solubilization temperature is lower than the sintering temperature) and from the control exerted by the second phase at the solubilization temperature. The limited amount of martensite is not significantly influencing material strength, although it is large enough to reduce its ductility, despite of the higher density.

Tab.6. Mechanical properties of 75F treated at 1200°C and of AISI 434L ferritic stainless steel.

material	density [g/cm^3]	HV0.01	UTS, [MPa]	y0.2, [MPa]	A, [%]	E, [J]
AISI 434L	6.81	200	254	176	5.9	40
75F treated at 1200°C	6.93	236	488	382	2.2	27

Solubilization at the other two temperatures increases microhardness, UTS and $\sigma y_{0.2}$, whilst elongation increases at 1100°C and slightly decreases at 1000°C.

As shown by Figure 10, microhardness increases due to the hardening of ferrite and martensite. A further increase in martensite content at 1000°C provides an additional contribution to hardening.

The mechanical properties of wrought dual phase steels are strongly influenced by the martensite amount and microhardness, and by the microstructure morphology, which depends on the rolling conditions and on heat treatment (intermediate quenching, intercritical annealing, step quenching) [6,8]. By Image Analysis, grain size and morphology have been evaluated, and the results are reported in Tab.7. Roundness of the grains is defined as $P^2/4\pi A$, where P and A are the perimeter and the area of the martensitic

grains in the metallographic section, respectively. Elongation is defined as D_{max}/D_{min}, where D_{max} and D_{min} are the maximum and the minimum Feret diameters of the ferritic grains, respectively.

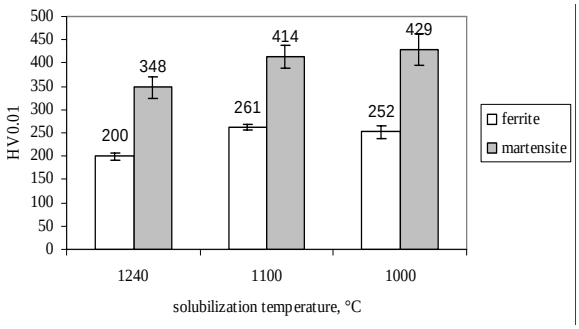

Fig.10. Microhardness of microstructural constituents in materials solubilized at different temperatures.

Tab.7. Microstructural details of the studied materials.

Material	Grain roundness	Grain elongation	Grain size [μm]
as-sintered	8.3	2.0	23
treated at 1100°C	4.5	2.2	22
treated at 1000°C	11	2.1	29

Table 7 shows that the three materials have similar microstructural features, with an appreciable difference in terms of roundness only. However, this difference is too small to influence mechanical properties that can be rather correlated to the martensite volume fraction and its microhardness. Tensile properties are plotted versus the product between martensite fraction and microhardness in Figs.11,12. The treatment at 1100°C does not significantly change the martensite content, but increases both strength and ductility, as a consequence of the micorstructural hardening (strength) and of the dissolution of the sigma phase (ductility). Treatment at 1000°C increases microhardness and martensite content by about 50 %, thus resulting in an increase in $\sigma_{y0.2}$ and a slight decrease in elongation. With respect to the steel treated at the higher temperature, UTS does not increase, since the increase in yield strength is compensated by the reduction in ductility. Tensile properties of the material solubilized at 1100°C are comparable to those of the low carbon sintered AISI 410 martensitic stainless steel.

Results of the instrumented impact tests are reported in Table 8, along with microhardness. Impact energy decreases after solubilization treatments, as shown in Fig.13, since the increase in microhardness and in the martensite fraction at 1000°C reduces deflection, Fig.14, i.e. the ability of the material to resist crack nucleation with an extensive plastic deformation. Both F_{max} and F_y are correlated to microhardness [9]. The different ductility of the material treated at 1100°C under tensile and impact loading is due to the effect of the strain rate which, as is well known, tends to increase brittleness.

Tab.8. Results of instrumented impact tests: F_{max} is the maximum load, F_y the load at general yielding, δ deflection [nostro lavoro].

Temperature [°C]	HV0.01	F_{max}, [kN]	F_y, [kN]	δ, [mm]	E, [J]
as sintered	217	18	13.2	1.4	21
1000	322	16.0	15	0.7	11
1100	284	14.8	13.9	0.8	12

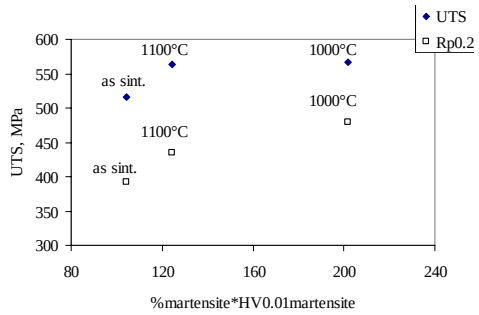

Fig.11. UTS and $\sigma_{y\,0.2}$ vs. (% martensite *HV0.01 martensite).

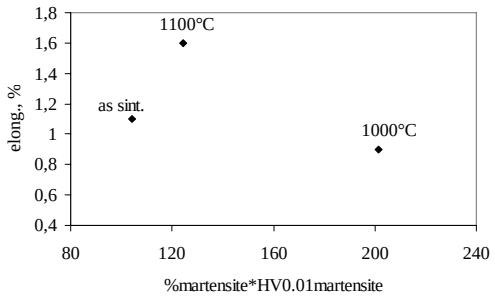

Fig.12. Elongation vs. (% martensite *HV0.01 martensite).

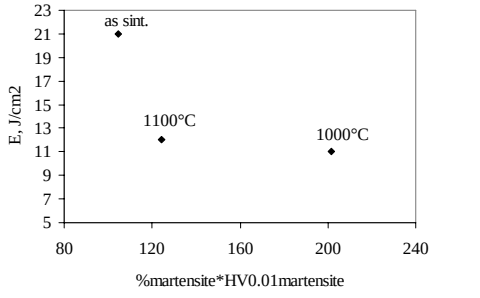

Fig.13. Impact energy vs. (% martensite *HV0.01 martensite).

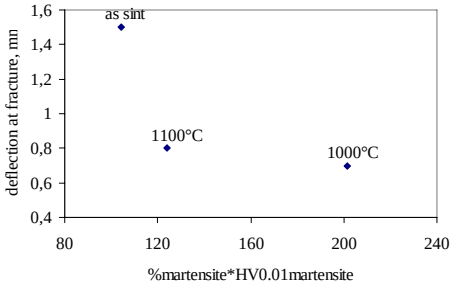

Fig.14. Deflection at fracture vs. (% martensite *HV0.01 martensite).

CONCLUSIONS

Dual phase stainless steels have been produced by sintering mixtures of 75 % ferritic powder and 25 % austenitic powder. Sintered microstructure comprises ferrite, martensite, (deriving from the destabilization of austenite) and sigma phase. This latter was eliminated by solubilization treatments conducted at 1000°C, 1100°C and 1200°C in an Ar atmosphere. After heat treatments, alloy microstructure displayed ferrite and martensite only. Moreover, it turned out that the higher the solubilization temperature the higher was, the ferrite content in the final products.

Mechanical properties depend on martensite content. In particular, the steel treated at 1200°C contains 95 % ferrite. It displays a higher strength and a lower ductility with respect to a typical ferritic stainless steel.

Among the steels heat-treated at different temperatures, the one solubilized at 1100°C has the better mechanical properties. Indeed, it posses higher strength and higher ductility than the as-sintered material, thanks to the microstructural hardening and the elimination of sigma phase. Contrarily, impact energy is lower than in the as-sintered material, although this material retains significant impact strength.

REFERENCES

[1] Marcu Puscas, T., Molinari, A., Kazior, J., Pieczonka, T., Nykiel, M.: Powder Metallurgy, vol. 44, 2001, no. 1, p. 48
[2] Kazior, J., Marcu Puscas, T., Pieczonka, T., Fedrizzi, L., Nykiel, M., Molinari, A.: Advances in Powder Metallurgy and Particulate Materials, vol. 7, 2000, p. 43
[3] German, R.: Powder Metallurgy Science, vol. 177, 1984, Princeton NJ, MPIF
[4] Miyakusu, K. et al. In: Proceedings of International Conference on Stainless Steels. 1991 June 10-13, Chiba, Japan, p. 585
[5] Maki, T.: Solid State &Materials Science, vol.2, 1997, no. 3, p. 290
[6] Kim, NJ., Thomas, G.: Metallurgical Transactions A, vol. 12, 1981, p. 483
[7] Sundman, B. et al.: Calphad, vol. 9, 1985, p. 153
[8] Davies, RG.: Metallurgical Transactions A, vol. 9, 1978, p. 671
[9] Molinari, A. et al. In: Proceedings PM2001, European Congress and Exhibition on Powder Metallurgy. Nice, 22-24 October 2001. Vol. 2. Shrewsbury : EPMA, p. 298